Photosynthesis Research **74:** 109–119, 2002.

Regular paper

Chlorophyll breakdown in spinach: on the structure of five nonfluorescent chlorophyll catabolites*

Joachim Berghold[1], Kathrin Breuker[1], Michael Oberhuber[1], Stefan Hörtensteiner[2] & Bernhard Kräutler[1,**]

[1]*Institute of Organic Chemistry, Leopold-Franzens-Universität Innsbruck, Innrain 52a, 6020 Innsbruck, Austria;* [2]*Institute of Plant Sciences, Universität Bern, Altenbergrain 21, 3013 Bern, Switzerland;* [**]*Author for correspondence (e-mail: bernhard.kraeutler@uibk.ac.at; fax: +43-512-5072892)*

Key words: chlorophyll, chlorophyll catabolism, mass spectrometry, NMR-spectroscopy, partial synthesis, tetrapyrrole

Abstract

In extracts of senescent leaves of spinach (*Spinacia oleracea*), five colourless compounds with UV/Vis-characteristics of nonfluorescent chlorophyll catabolites (NCCs) were detected and tentatively named *So*-NCCs. The most abundant polar NCC in the leaves of this vegetable, *So*-NCC-2, had been isolated earlier and its constitution was determined by spectroscopic means. The catabolite *So*-NCC-2 was found to be an epimer of a polar NCC from barley (*Hordeum vulgare*), the first non-green chlorophyll catabolite from a higher plant to be structurally analyzed. Here, we report on the isolation of four additional *So*-NCCs from the extracts of senescent leaves of *Sp. oleracea* by two- (or multi-)stage chromatographic purification and on their structural characterization. The constitution of *So*-NCC-3 could be determined by spectroscopic analysis in combination with chemical correlation with a known NCC from *Cercidiphyllum japonicum* (*Cj*-NCC): *So*-NCC-3 was identified as the hydrolysis product of the methyl ester function of *Cj*-NCC. The less polar catabolite *So*-NCC-4 could be directly identified with *Cj*-NCC. Two further *So*-NCCs, *So*-NCC-1 and *So*-NCC-5, were detected only in trace amounts. Five structurally related nonfluorescent chlorophyll catabolites (*So*-NCCs) are thus present in senescent leaves of spinach. The structures of this set of *So*-NCCs indicate several peripheral refunctionalization reactions and inform on the late catabolic transformations during leaf senescence. The transformation of the tetrapyrrolic skeleton in chlorophyll catabolism in spinach and in *C. japonicum* is revealed to exhibit a common stereochemical pattern.

Introduction

Chlorophyll breakdown in degreening plants has always been a phenomenon of general interest (see e.g. Mendel 1865; Hendry et al. 1987; Brown et al. 1991). However, only about 10 years ago have de-greened products of chlorophyll breakdown been discovered (Matile 1987; Kräutler et al. 1991; Matile et al. 1996; Kräutler and Matile 1999), in spite of the fact that an estimated 1000 million tons of chlorophyll are degraded annually on earth (see Brown et al. 1991). The first of the non-green chlorophyll catabolites from higher plants to be structurally characterized was *Hv*-NCC-1 (**1**, see Figure 1), a polar 'nonfluorescent' chlorophyll catabolite (NCC) from senescent primary leaves of barley (*Hordeum vulgare*) (Bortlik et al. 1990; Kräutler et al. 1991, 1992). The constitution of **1** showed it to be structurally related to chlorophyll *a* (**2a**) and gave first clues on the major transformations responsible for the colour changes that occur in chlorophyll breakdown in plants (Matile and Kräutler 1995).

In the meantime, half a dozen NCCs from higher plants have been detected and analyzed structurally, among them the *Bn*-NCCs (**3a**, **3b**, **3c**) from oilseed rape (*Brassica napus*) (Ginsburg et al. 1992; Mühlecker et al. 1993; Mühlecker and Kräutler 1996)

* Dedicated to Prof. Philippe Matile on the occasion of his 70th birthday.

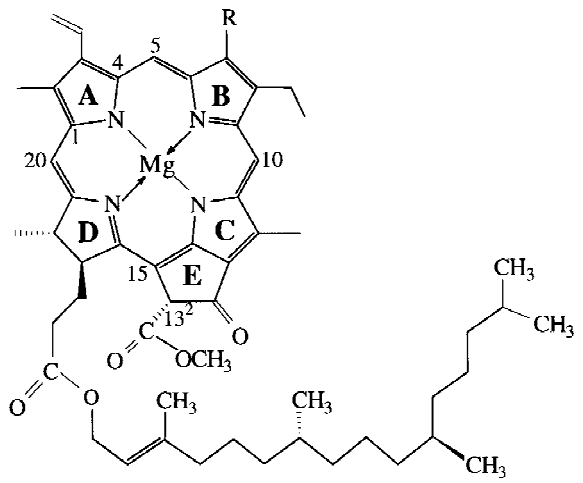

2a: chlorophyll a (R = CH_3)
2b: chlorophyll b (R = HC=O)

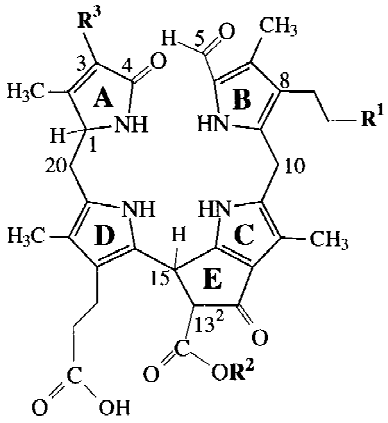

1: *Hv*-NCC-1; R^1 = OH, R^2 = CH_3; R^3 = CH(OH)-CH_2OH
3a: *Bn*-NCC-1; R^1 = O-malonyl; R^2 = H; R^3 = CH=CH_2
3b: *Bn*-NCC-2; R^1 = O-β-glucopyranosyl; R^2 = H; R^3 = CH=CH_2
3c: *Bn*-NCC-3; R^1 = OH; R^2 = H; R^3 = CH=CH_2
4: *Cj*-NCC; R^1 = OH; R^2 = CH_3; R^3 = CH=CH_2
5: *So*-NCC-2; R^1 = OH; R^2 = CH_3; R^3 = CH(OH)-CH_2OH
6: *So*-NCC-3; R^1 = OH; R^2 = H; R^3 = CH=CH_2
7: *So*-NCC-4; R^1 = OH; R^2 = CH_3; R^3 = CH=CH_2
8: *So*-NCC-5; R^1 = H; R^2 = CH_3; R^3 = CH=CH_2
9: *So*-NCC-1; R^1 = OH; R^2 = H; R^3 = CH(OH)-CH_2OH

Figure 1. Structural formulae of chlorophyll *a* and *b* (**2a**, **2b**); constitutional formulae of the nonfluorescent chlorophyll catabolites (NCCs): *Hv*-NCC-1 (**1**, from barley, *Hordeum vulgare*), *Bn*-NCC-1 (**3a**), *Bn*-NCC-2 (**3b**), *Bn*-NCC-3 (**3c**, all from oilseed rape, *Brassica napus*), *Cj*-NCC (**4**, from *Cercidiphyllum japonicum*), *Ls*-NCC (**4′**, from sweet gum, *Liquidambar styraciflua*) and of the *So*-NCCs from spinach (*Spinacia oleracea*): *So*-NCC-1 (**9**), *So*-NCC-2 (**5**), *So*-NCC-3 (**6**), *So*-NCC-4 (**7**) and *So*-NCC-5 (**8**). The atoms of all of the listed tetrapyrroles are numbered according to the IUPAC numbering of the chlorophylls (see e.g. Scheer 1991).

and an NCC (with a common constitution) from *Cercidiphyllum japonicum* (*Cj*-NCC, **4**) (Curty and Engel 1996) and from *Liquidambar styraciflua* (Iturraspe et al. 1995) (see Figure 1). All NCCs exhibit the same basic structural pattern, which was discovered in **1**. The surprising lack of NCCs that carry a formyl group at position 7, i.e. that are more closely related to chlorophyll *b* (**2b**), meanwhile can be explained by the existence of reductases that reduce chlorophyll(ide) *b* to chlorophyll(ide) *a*, prior to further breakdown (Ito et al. 1993, 1996; Scheumann et al. 1996, 1999; Kräutler and Matile 1999). The tetrapyrrolic NCCs are deposited into the vacuoles of the senescent leaf (Matile et al. 1988; Hinder et al. 1996) and have been suggested to represent the final stages of senescence based chlorophyll catabolism in higher plants (Matile et al. 1996; Kräutler and Matile 1999; Hörtensteiner and Kräutler 2000). However, an urobilinogenic chlorophyll catabolite was recently obtained from isolates from senescent primary leaves of barley and was suggested to be the result of an oxidative loss of the formyl group of **1** (Losey and Engel 2001).

We have recently started to investigate chlorophyll breakdown in spinach (*Spinacia oleracea*) and have reported on the detection, isolation and structural characterization of *So*-NCC-2 (**5**), the major polar NCC from naturally degreened leaves of this vegetable (Oberhuber et al. 2001). The catabolite *So*-NCC-2 (**5**) was identified as a stereoisomer of *Hv*-NCC-1 (**1**). Here we report on three less polar NCCs (*So*-NCC-3 (**6**), *So*-NCC-4 (**7**) and *So*-NCC-5 (**8**)), as well as on a more polar *So*-NCC (*So*-NCC-1 (**9**)) from spinach.

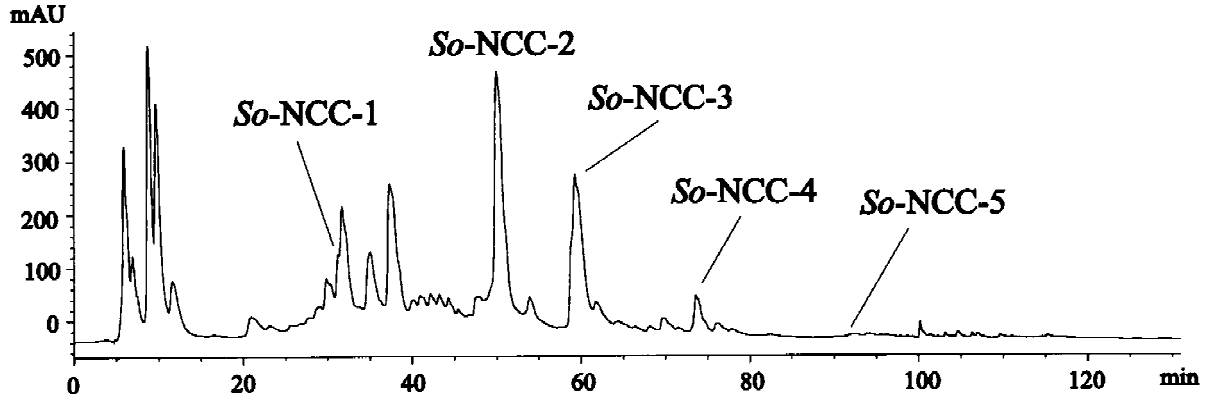

Figure 2. Analytical HPLC trace (recorded at λ=320 nm) of the raw extract of senescent spinach leaves, obtained as described in 'Materials and methods' (see section 'Isolation of *So*-NCCs').

Materials and methods

Reagents used were reagent-grade commercials and distilled before use. Reagents and HPLC solvents were from Fluka (Buchs, Switzerland) and from Merck (Darmstadt, Germany). TLC: analytical (0.25 mm silica gel 60 F_{254}) and preparative (20 cm×20 cm, 1 mm silica gel 60 F_{254}) TLC plates were from Merck, Darmstadt, Germany. Sep-Pak-C18 cartridges were from Waters Associates. Analytical and preparative HPLC: solvent gradient is given in the text as: time in min. (V% water/V% 100 mM K-phosphate buffer pH=7.0/V% methanol) HPLC (HP 1100); vacuum degasser, manual sampler, diode array detector, analytical column: Hypersil ODS 5 μm, 250×4.6 mm i.d. (Thermoquest), solvent gradient: 0 min (0/80/20), 10 min (0/80/20), 70 min (0/40/60), 80 min (0/40/60), 82 min (20/20/60), 87 min (20/10/70), 90 (15/5/80); flow: 0.5 ml/min; preparative column: Hypersil ODS 5 μm, 250×21.2 mm i.d. (Thermoquest); All chromatograms were taken at r.t. and data was processed by HP Chemstation for 3D. UV/Vis-Spectra: Hitachi-U3000 spectrophotometer; λ_{max}(nm)/(log ε resp. rel ε). CD Spectra: Jasco-J715 spectropolarimeter; λ_{max}(nm) and λ_{min}(nm)/($\Delta\varepsilon$). NMR Spectra: Varian Unity$_{plus}$ 500 or Bruker AM-300 $\delta(C^1HD_2OD)$=3.31 ppm and $\delta(^{13}CD_3OD)$=49.0 ppm, $\delta(HDO)$=4.79 ppm) (see e.g. Pretsch et al. 2000). MS: Finnigan MAT 95-S positive-ion mode; FAB-MS: cesium gun, 20 keV, matrix: glycerol; ESI-MS: flow rate 300 nl/min; spray voltage 1.2 kV, solvents: water/MeOH mixtures (1:1).

Isolation of So-*NCCs*

Senescent leaves of spinach (*Spinacia oleracea*) were obtained as described earlier (Oberhuber et al. 2001). An extract of the NCCs was obtained by mixing and suspending 58.7 g of the ground leaf tissue once in 120 ml and three times with 60 ml of 20 mM K-phosphate buffer (pH 7.0)/MeOH (1:1 v/v), followed each time by centrifugation (5 min at 10 000×g) and separation of the supernatants. The combined supernatants were diluted (1:1) with 300 ml of methanol and centrifuged once more. The resulting supernatant was then concentrated under reduced pressure, lyophilized and dissolved in 20 ml water. The analytical HPLC trace at 320 nm of this aqueous solution is shown in Figure 2. Using preparative HPLC this yellow solution was separated (Hypersil ODS, MeOH/K-phosphate buffer, pH 7.0, with a gradient: 0 min (0/80/20), 10 min (0/80/20), 70 min (0/40/60), 80 min (0/40/60), 82 min (20/20/60), 87 min (20/10/70), 90 (15/5/80); flow rate 5 ml/min; UV detection at 320 nm).

Detection and preliminary characterization of So-*NCC-1 (***9***)*

The fraction at 42–44 min retention time, containing *So*-NCC-1 (**9**) was desalted by the help of a Waters Sep-Pak-C18 cartridge and purified by a second round of preparative HPLC (isocratic: methanol/0.1 M K-phosphate, pH 7.0, 3:1 (v/v)). The fraction of *So*-NCC-1 (**9**) at 51–56 min was desalted by Waters Sep-Pak-C18 cartridge and had the following spectroscopic properties: UV/Vis (60 mM K-phosphate buffer pH 7.0 in H_2O/MeOH 60/40) λ_{max} (nm)/(rel ε)=243sh

(0.85), 273 (0.70), 316 (1.0). ESI-MS (*m/z* (%)): 667.3 (25), 666.3 (83), 665.3 (100, $[M+H]^+$); 648.3 (12), 647.3 (17, $[M-H_2O+H]^+$); 622.3 (6), 621.3 (5, $[M-CO_2+H]^+$); 510.2 (10), 509.2 (26), 508.2 (31, [M−ring A+H]$^+$); 465.2 (11), 464.2 (12, [M−ring A-CO_2+H]$^+$).

So-*NCC-2 (**5**)*

A sample of 10.1 mg (14.9 μmol) of the catabolite *So*-NCC-2 (**5**) was obtained from the fraction with retention time at 61–63 min, as described earlier (Oberhuber et al. 2001). Analytical HPLC of **5**: 50.5 min retention time.

So-*NCC-3 (**6**)*

From the HPL-chromatographic separation, described above, the fraction of *So*-NCC-3 (**6**), obtained at 68–70 min retention time, was diluted 1:1 with water (ca. 15 ml), applied to a Waters Sep-Pak-C18 cartridge. The loaded cartridge was washed with water to remove the buffer, and with MeOH, to elute the slightly yellow fraction of **6**. The solvents of the collected eluates with **6** were removed *in vacuo* and the residue dissolved in about 1.5 ml of HPLC-eluent (MeOH/0.1 M K-phosphate, pH 7.0, 3:2 (v/v)) and purified by a second run of preparative HPLC. The fraction with a retention time of 66–70 min was collected, desalted with a Waters Sep-Pak-C18 cartridge, the residue was dissolved in 1.5 ml of HPLC-eluent (MeOH/0.1 M K-phosphate, pH 7.0, 4:1 (v/v)) and purified by a third run of preparative HPLC (gradient: 0 min (0/80/20), 10 min (0/80/20), 15 min (0/53/47), 80 min (0/53/47). The *So*-NCC-3 fraction (retention time 41–44 min) was collected, diluted 1:1 with water and the residual solution was applied to a Sep-Pak-C18 cartridge. After washing with H_2O (20 ml), *So*-NCC-3 (**6**) was eluted with methanol and the eluate was dried (at high vacuum) at $T < 0°$, yielding 0.5 mg (0.8 μmol) of *So*-NCC-3 (**6**). Analytical HPLC of **6**: 60.7 min retention time. Spectroscopic Data: UV/VIS (H_2O) λ_{max}(nm)/(rel ε)=240sh (1.17), 316 (1.0); CD (H_2O, c=2.5 10^{-5} M) $\lambda_{min/max}$(nm)/($\Delta\varepsilon$)=225 (14.63), 252 (−3.61), 280 (−14.13), 320 (5.53). ^{1}H-NMR (500 MHz, 26 °C, D_2O): 1.89 (s, $H_3C(18^1)$); 1.94 (s, $H_3C(2^1)$); 2.16 (s, H_3C (12^1)); 2.19 (s, $H_3C(7^1)$); 2.27 (m, H_2C (17^2)); 2.57 (m, $H_AC(20)$); 2.70–2.60 (m, H_2C (8^1) and H_2C (17^1)); 2.86 (m, $H_BC(20)$); 3.55 (m, $H_2C(8^2)$); 3.70 (broad, $HC(13^2)$); 4.00 (m, HC(1) and $H_2C(10)$); 4.70 (s, 1H, HC(15)); 5.45 (d, J=11.7 $H_{cis}C(3^2)$); 5.88 (d, J=19.5 $H_{trans}C(3^2)$); 6.42 (dd, J=11.7, 19.5, $HC(3^1)$); 9.14 (s, HC(5)). FAB-MS (glycerol matrix; *m/z* (%)): 671.3 (20), 670.4 (33), 669.3 (63, $[M+K]^+$); 633.3 (17), 632.3 (43), 631.3 (100, $[M+H]^+$); 626.0 (15), 625.2 (38, $[M-CO_2+K]^+$); 508.2 (24, [M−ring A+H]$^+$); 464.2 (19, [M−ring A−CO_2+H]$^+$). HR-FAB-MS $[M+H]^+$: 631.277±0.005 ($C_{34}H_{39}N_4O_8$; calc. 631.277).

So-*NCC-4 (**7**)*

From the HPL-chromatographic separation, described above, the fraction of *So*-NCC-4 (**7**), obtained at 82–85 min retention time, was diluted 1:1 with water (ca. 15 ml) and desalted on a Waters Sep-Pak-C18 cartridge. The solvents of the collected eluates with **7** were removed *in vacuo* and the residue dissolved in about 1.5 ml of HPLC-eluent (MeOH/0.1 M K-phosphate, pH 7.0, 4:1 (v/v) and purified in a second run of preparative HPLC (gradient: described at isolation of NCCs). The fraction with *So*-NCC-4 (retention time 78–80 min) was collected, diluted 1:1 with water and the residual solution was applied to a Sep-Pak-C18 cartridge. After washing with H_2O (20 ml), **7** was eluted with MeOH and the eluate was dried under high vacuum at $T < 0°$. The remaining reside was dissolved in 2 ml methylene chloride, precipitated with 10 ml *n*-Hexan and followed centrifugation (5 min at 10 000×*g*). The pellet was dried at high vacuum at $T < 0°$, yielding 0.12 μmoles of *So*-NCC-4 (**7**). Analytical HPLC of **7**: 72.2 min retention time. Spectroscopic data: UV/VIS (H_2O) λ_{max}(nm)/(rel. ε)=245sh (1.13), 315 (1.00); CD (H_2O, c=2.5 10^{-5} M) $\lambda_{min/max}$(nm)/($\Delta\varepsilon$)=224 (25.13), 251 (6.42), 282 (−16.37), 322 (6.34). FAB-MS (glycerol matrix; *m/z* (%)): 685.3 (12), 684.3 (41), 683.3 (35, $[M+K]^+$); 647.3 (16), 646.3 (48), 645.3 (92, $[M+H]^+$); 614.3 (12), 613.3 (19, [M−CH_3OH+H]$^+$); 524.2 (21), 523.2 (44); 522.2 (100, [M−ring A+H]$^+$); 491.2 (26); 490.2 (25, [M−ring A−CH_3OH+H]$^+$); 462.2 (7, [M−ring A−CH_3OH−CO+H]$^+$). HR-FAB-MS $[M+H]^+$: 645.290±0.005 ($C_{35}H_{41}N_4O_8$; calc. 645.292). The ^{1}H-NMR spectrum of this sample of *So*-NCC-4 (**7**) was consistent with the suggested structure, but indicated the presence of small amounts of impurities, which could not be separated by HPLC.

Direct isolation of So-*NCC-4 (**7**)*

A total of 70 g of senescent leaves of *Spinacia oleracea* (after onset of flowering) were mixed for 2

min in 1000 ml acetone/methanol (v/v, 1:1) using a Braun Vario-Mixer. The slurry was filtered through a cellite filter and washed with 1000 ml of the same solvent mixture. The green solution was concentrated to 200 ml by evaporation of the solvent at room temperature, and diluted with 1000 ml water. After five-fold extraction, using each time 250 ml methylene chloride, the organic phase was collected, dried by calcium chloride, and the solvent was evaporated. The residue was dissolved in 4 ml methylene chloride, applied to three silica gel 60 thin layer plates and developed in chloroform/methanol/water (v/v/v, 95/10/1). The silica gel zone containing the catabolite, which has the same retention as *Cj*-NCC, was extracted by 100 ml methylene chloride/methanol (v/v, 7/3), washed with 100 ml 100 mM potassium phosphate buffer pH=5.2, and filtered through a cotton plug. The solvent was evaporated, and the residue was dissolved in 4 ml HPLC-eluent (MeOH/0.1 M K-phosphate, pH 7.0, 3:2 (v/v), followed by purification using preparative HPLC (gradient: 0 min (0/60/40), 84 min (0/60/40), 85 min (0/40/60)). The fraction of *So*-NCC-4 (**7**) (retention time 78–80 min) was collected, diluted 1:1 with water and applied to a Sep-Pak-C18 cartridge. After washing with H_2O (20 ml), *So*-NCC-4 was eluted with methanol and the eluate was dried (at high vacuum) at $T < 0°$. The reside was dissolved in 2 ml methylene chloride, precipitated with 10 ml *n*-hexane, and centrifuged 5 min at $10\,000 \times g$. The pellet was dried at high vacuum at $T < 0°$, yielding 0.3 mg (0.5 μmoles) of pure *So*-NCC-4 (**7**), with the following spectroscopic properties: UV/VIS (H_2O) λ_{max}(nm)/(rel. ε)=242sh (1.13), 315 (1.00); ^{1}H-NMR (500 MHz, 26 °C, CD_3OD): 1.89 (s, $H_3C(18^1)$); 1.91 (s, $H_3C(2^1)$); 2.05 (s, $H_3C(12^1)$); 2.20 (s, $H_3C(7^1)$); 2.28 (m, $H_2C(17^2)$); 2.58 (m, $H_AC(20)$); 2.72 (m, $H_2C(8^1)$ and $H_2C(17^1)$); 2.81 (dd, J=14.6, 4.9 , $H_BC(20)$); 3.57 (m, $H_2C(8^2)$); 3.70 (broad, $HC(13^2)$); 3.90 (m, HC(1) and $H_2C(10)$); 4.84 (s, 1H, HC(15)); 5.30 (dd, J=11.6, 1.8 $H_{cis}C(3^2)$); 5.88 (d, J=17.7, 2.4 $H_{trans}C(3^2)$); 6.40 (dd, J=11.6, 17.7, $HC(3^1)$); 9.30 (s, HC(5)); ESI-MS (*m/z* (%)): 668.3 (4), 667.3 (10, $[M+Na]^+$); 647.3 (8), 646.3 (40), 645.3 (100, $[M+H]^+$); 614.3 (4), 613.3 (12, $[M-CH_3OH+H]^+$); 522.3 (5, [M−ring A+H]$^+$).

So-*NCC-5 (***8***)*

All non-green catabolites other than *So*-NCC-4 were also eluted from the silica plate used for the isolation of *So*-NCC-4 (**7**) with 100 ml methanol. The solvent was evaporated, and the dried material re-dissolved in 5 ml methanol, followed by analytical HPLC analysis. Based on retention times and UV spectral data, *So*-NCC-2, *So*-NCC-3, and *So*-NCC-4 were identified among the eluents. A further fraction with a UV spectrum typical for NCCs was eluted at 92 min retention time and was purified by preparative HPLC (gradient: 0 min (0/40/60), 15 min (0/40/60), 17 min (20/20/60), 20 min (25/10/65)). *So*-NCC-5 (**8**) was collected at a retention time of 37–41 min and the resulting sample of **8** had the following spectroscopic data: UV/Vis (10 mM K-phosphate buffer pH 7.0 in H_2O/MeOH 35/65) λ_{max}(nm)/(rel. ε)=242sh (1.3), 317 (1.0). ESI-MS (*m/z* (%)): 630.3 (38), 629.3 (100, $[M+H]^+$); 598.3 (12), 597.3 (31, $[M-CH_3OH+H]^+$).

Cj-*NCC (***4***)*

This NCC was isolated from senescent leaves of *Cercidiphyllum japonicum* as described (Curty and Engel 1996; Oberhuber et al. 2001). By analytical HPLC *Cj*-NCC (**4**) had at a retention time of 72.2 min.

Partial hydrolysis of Cj-*NCC (***4***) and preparation of the di-acid (***6a***)*

A sample of 4 mg of *Cj*-NCC (**4**) from senescent leaves of *C. japonicum* was disolved in 5 ml DMSO and mixed with 4 mg esterase from porcine liver (Sigma, activity 41 U/mg) disolved in 40 ml 100 mM K-phosphate buffer, pH=7.9, and 5 ml acetonitrile were added to this mixture. After 1 week of incubation at 40 °C, 20% conversion of **4** into a diacid were detected by analytical HPLC (method described in the section 'Isolation of NCCs from spinach'). Subsequently, the pH of the NCC/esterase solution was adjusted to pH 5.2 by addition of solid potassium dihydrogen phosphate, followed by twofold extraction of the catabolites with methyl acetate. The organic layers were collected, diluted 1:1 with methylene chloride, filtered though cellulose and evaporated to dryness yielding 0.3 mg (0.5 μmol) of diacid (**6a**), which had UV/VIS and ^{1}H-NMR spectra identical with those of *So*-NCC-3 (**6**). Analytical HPLC of **6a**: 60.5 min retention time. ESI-MS (*m/z* (%)): 633.3 (28), 632.3 (83), 631.3 (100, $[M+H]^+$); 615.3 (11), 614.3 (35), 613.3 (45, $[M-H_2O+H]^+$); 588.3 (11), 587.3 (12, $[M-CO_2+H]^+$); 509.2 (15), 508.2 (18, [M−ring A+H]$^+$); 465.2 (11), 464.2 (13, [M−ring A−CO_2+H]$^+$).

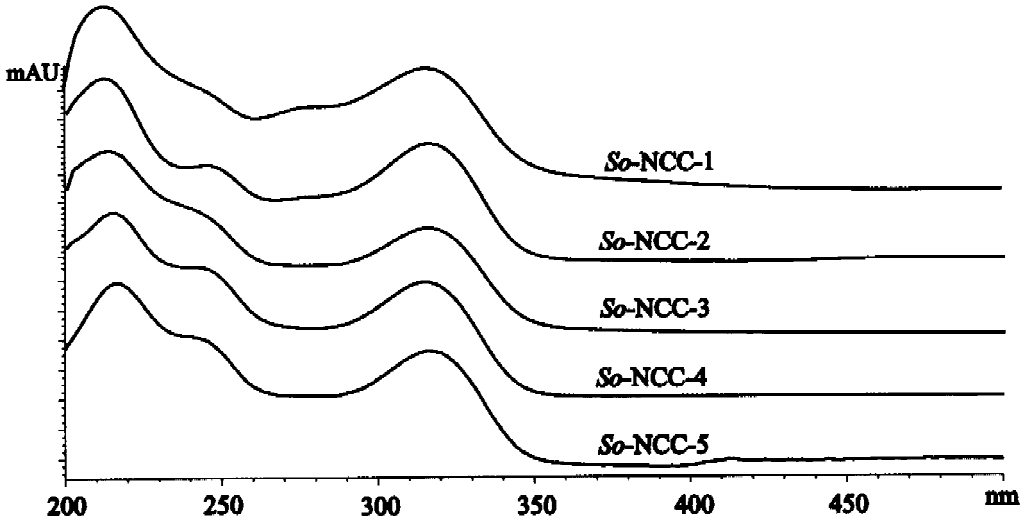

Figure 3. UV/Vis-spectra of the *So*-NCCs recorded during analytical HPLC with the diode array detector as in Figure 2 at retention times 31 min (*So*-NCC-1), 50 min (*So*-NCC-2), 60 min (*So*-NCC-3), 73 min (*So*-NCC-4), and from preparative HPLC purification of *So*-NCC-5, as described in 'Materials and methods'.

Results and discussion

Based on the characteristic UV-absorbance properties of NCCs (Mühlecker and Kräutler 1996; Kräutler and Matile 1999) and using analytical HPLC, five polar, colourless and nonfluorescent chlorophyll catabolites (NCCs) could be tentatively identified in senescent leaves of flowering spinach plants (*Spinacia oleracea*) (see Figure 2). The isolation and structural analysis of the most abundant of these, of *So*-NCC-2 (**5**), has been described recently (Oberhuber et al. 2001): from 58.7 g (wet weight) of senescent leaves of flowering spinach plants 10.1 mg (ca. 14.9 μmol) of the polar *So*-NCC-2 (**5**) were isolated by a two-stage purification procedure based on HPLC. The catabolite **5**, which represented about 20% of the chlorophyll present in the intact leaves, was obtained as a ca. (1:10)-mixture of two fractions, that equilibrated slowly in neutral aqueous solution (see below). The catabolite *So*-NCC-2 (**5**) was shown to have the same constitution as *Hv*-NCC-1 (**1**), the polar catabolite from primary leaves of barley that had been artificially degreened in darkness. From HPLC-analysis, the two catabolites (**1** and **5**) clearly were shown to be non-identical (see Oberhuber et al. 2001). Their epimeric relationship could be deduced to be due to a stereochemical difference at C(1), introduced into the catabolites in a stereochemically divergent reduction step in the course of chlorophyll breakdown. In support of this proposal, the catabolite from spinach (*So*-NCC-2, **5**) was identified with a product of the chemical dihydroxylation (with osmium tetroxide) of the NCC from *C. japonicum* (*Cj*-NCC, **4**) (Oberhuber et al. 2001).

The present report concerns the identification of three less polar NCCs (*So*-NCC-3 (**6**), *So*-NCC-4 (**7**) and *So*-NCC-5 (**8**)) in the degreened leaves of spinach, and their structural characterization. In addition a further colourless and rather polar compound from spinach (*So*-NCC-1, **9**) is tentatively characterized and identified as an NCC.

When working up 58.7 g (wet weight) of senescent leaves of flowering spinach plants [the original batch used for the identification of *So*-NCC-2 (**5**) (Oberhuber et al. 2001)], the two new catabolites *So*-NCC-3 (**6**) and *So*-NCC-4 (**7**) could be tentatively identified in two fractions less polar than that of *So*-NCC-2 (**5**) (i.e. at higher retention times in reversed phase HPLC, see Figure 2). The UV/Vis-spectra of **6**, **7** and **8** matched those of **1** (see Kräutler et al. 1992) and **5** (see Figure 3). The long wavelength part of these spectra is due to the α-formyl-pyrrole moiety (ring B). In agreement with the slightly differing α-formyl-pyrrole moieties in **6** and in **8**, the absorbance maximum at longest wavelength in the spectrum of **8** occurred at 317 nm, i.e. 2 nm bathochromic compared to that of **6**. The CD spectra of the catabolites **6** and **7** were nearly congruent also and matched that of **5**, suggesting the stereogenic centres C(15) and C(1) to have the same configurations in **5**, **6** and **7** (see below).

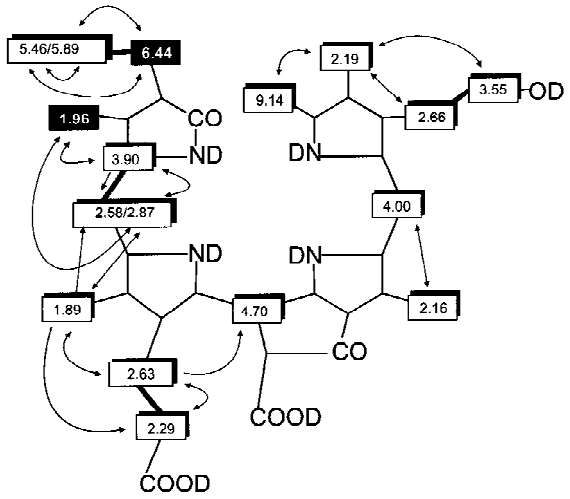

Figure 4. ^{1}H-NMR chemical shift data of *So*-NCC-3 (**6**). Signal assignments of carbon-bound hydrogen atoms of **6** (solid arrows represent ROESY correlations; bold lines indicate TOCSY correlations) and qualitative comparison of the chemical shift values of **6** with the corresponding values for *Bn*-NCC-3 (**3c**) (from Mühlecker and Kräutler 1996, but referenced to δ(HOD)=4.79 ppm), where light and (two) black boxes indicate chemical shift values that differ by less or by more than 0.1 ppm, respectively.

The catabolite *So*-NCC-3 (**6**) was isolated by two further purification steps based on preparative HPLC and a chromatographically pure sample of 0.5 mg (0.8 μmol) of **6** was obtained in this way. The molecular formula of *So*-NCC-3 (**6**) was determined as $C_{34}H_{38}N_4O_8$ by high resolution fast atom bombardment (FAB) mass spectrometry in (+)-ion mode (reviewed in Watson 1995): the experimental peak of the pseudo-molecular ion $[M+H]^+$ was observed at *m/z*=631.277±0.005. The same molecular formula was previously derived from the mass spectrum of *Bn*-NCC-3 (**3c**) (Mühlecker and Kräutler 1996). In the spectra of both (**6** and **3c**) loss of 44 mass units (due to a decarboxylation reaction) as well as loss of 123 mass units (due to ring A) from $[M+H]^+$ were deduced from the characteristic fragments (Mühlecker and Kräutler 1996). The signals of 33 of the 39 protons were detected in 500 MHz ^{1}H-NMR spectra of **6** in D_2O: one singlet (at low field) for the formyl proton and four singlets (at high field) for the four methyl groups attached at the β-pyrrole positions; however, a singlet near 3.7 ppm (due to a methyl ester function) was lacking. In addition, the typical pattern for an unsubstituted peripheral vinyl group was detected in the chemical shift range near 6 ppm. The remaining oxygen atom was assigned according to the typical downfield shift of the hydrogen atoms $H_2C(8^2)$ to a hydroxy group at this peripheral substituent. According to this analysis the constitution of *So*-NCC-3 (**6**) was suggested to be identical with that of *Bn*-NCC-3 (**3c**). To further characterize the structure of catabolite **6**, it was compared to the di-acid **6a** obtained from hydrolysis of *Cj*-NCC (**4**) by pig liver esterase. To prepare **6a**, the catabolite *Cj*-NCC (**4**) (Curty and Engel 1996) was dissolved in a buffered aqueous solution of pig liver esterase (as described in Experimental). After about 170 h incubation at 40 °C, about 20% of **4** was converted into the more polar compound **6a**, which was isolated and then identified (by HPLC, mass spectrometry, and ^{1}H-NMR spectroscopy) with the diacid **6**. The spatial relationship between the carbon bound hydrogens of **6** could be derived from ROESY and TOCSY spectra (Sanders et al. 1987; Kessler et al. 1988). The derived chemical shifts for the signals in the ^{1}H-NMR spectra indicated *So*-NCC-3 (**6**) not to be identical with *Bn*-NCC-3 (**3c**), but rather to be a C(1)-epimer of it (see Figure 4).

Likewise, a sample of the catabolite *So*-NCC-4 (**7**) was isolated by two further preparative HPLC purification steps, and a chromatographically pure sample of about 0.12 μmoles of **7** was obtained in this way. Analytical HPLC and an FAB mass spectrum tentatively indicated *So*-NCC-4 (**7**) to have the same structure as *Cj*-NCC (**4**). To obtain a larger sample of **7**, the extracts of 70 g of senescent leaves from flowering spinach were purified by thin layer chromatography, as described for the isolation of *Cj*-NCC (Curty and Engel 1996). In this way, a sample of 0.3 mg of pure *So*-NCC-4 (**7**) was obtained, which was further analysed by FAB-mass spectrometry as well as ^{1}H-NMR spectroscopy, as follows: The molecular formula of *So*-NCC-4 (**7**) again was derived by high resolution FAB mass spectrometry in (+)-ion mode and was determined as $C_{35}H_{40}N_4O_8$ (experimental base peak $[M+H]^+$ at *m/z*=645.290±0.005). The same molecular formula was previously derived for *Cj*-NCC (**4**) (Curty and Engel 1996). In the spectra of both (**4** and **7**), loss of 123 mass units was also observed, due to loss of ring A observed as a characteristic fragmentation in the mass spectra of NCCs (Mühlecker et al. 1993; Mühlecker and Kräutler 1996). Indeed, *So*-NCC-4 (**7**) could be identified by HPLC, FAB-mass spectrometry and by comparison of the 1H-NMR spectra with the catabolite *Cj*-NCC (**4**) from *C. japonicum*.

A further rather unpolar fraction with UV-characteristics typical of NCCs (see Figure 3) could be obtained by HPLC of the raw mixture of NCCs

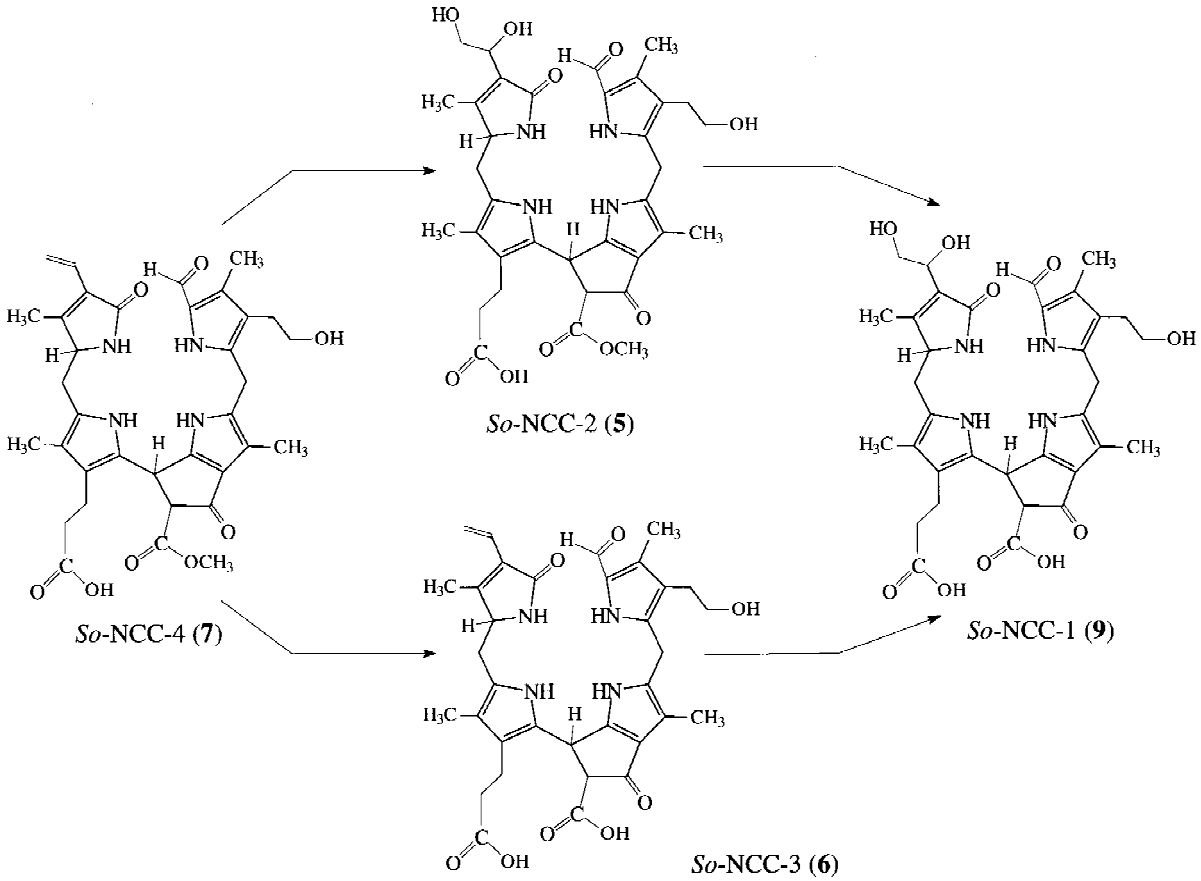

Figure 5. Likely parallel paths during late refunctionalization of the periphery of *So*-NCCs during chlorophyll breakdown in spinach.

(scratched-off the thin layer plates used for the isolation of *So*-NCC-4 (**7**)). The fraction of this less polar NCC, *So*-NCC-5 (**8**) was analysed by electrospray ionization (ESI) mass spectrometry (reviewed by Smith et al. 1995). Its pseudo-molecular ion $[M+H]^+$ appeared at *m/z*=629.3, i.e. at the same mass as that of the primary fluorescent chlorophyll catabolites (pFCCs) (Mühlecker et al. 1997, 2000). The UV-spectrum of the small fraction of **8** exhibited the characteristics of the spectra of an NCC. The catabolite *So*-NCC-5 (**8**) is, accordingly, tentatively assigned the structure of an NCC that is not yet refunctionalized at its periphery.

From re-chromatography of a very polar fraction with an absorbance maximum at 316 nm, a sample of a presumed *So*-NCC was isolated (tentatively named *So*-NCC-1, **9**), whose ESI mass spectrum showed a pseudo-molecular ion at *m/z*=665.3, i.e. with 14 mass units less than that of the less polar catabolite *So*-NCC-2 (**5**). Collisionally activated dissociation of $[M+H]^+$ yielded fragment ions at *m/z*=621.3, 508.2 and 464.2, indicating decarboxylation, loss of the ring A moiety and a combination thereof, respectively. These mass spectrometric data are consistent with the presence of a dihydroxy-ethyl side chain at ring A of *So*-NCC-1 (**9**), which then would (formally) be the product of the hydrolysis of the ester function of *So*-NCC-2 (**5**), in agreement with its high polarity.

Evidence for the presence of (at least) five *So*-NCCs is presented here, which represent an amount corresponding to about 25–40% of the chlorophyll originally present in the green leaves. The strongly differing polarity of the *So*-NCCs is reflected in the broad range of HPLC retention times on a stationary phase with low polarity: *So*-NCC-1: 32 min, *So*-NCC-2: 50 min, *So*-NCC-3: 61 min, *So*-NCC-4: 72 min, *So*-NCC-5: 92 min. A close structural relationship is revealed here for these five *So*-NCCs: starting with the apolar NCC (*So*-NCC-5, **8**), that is tentatively assigned to lack all peripheral refunctionalizations, and the more polar *So*-NCC-4 (**7**), which exhibits the in-

triguing hydroxylation at the inactivated β-position of the ethyl group at ring B, typical of all the NCCs previously found. The more polar NCCs, *So*-NCC-3 (**6**) and *So*-NCC-2 (**5**), then may come about from **7** either by a dihydroxylation of the vinyl group at ring A or by hydrolysis of the methyl ester function at ring E. Since both of these two NCCs (**5** and **6**) are both rather abundant in the senescent leaves of spinach, the availability of two relevant parallel catabolic pathways may be indicated at the stage of the *So*-NCCs (see Figure 5). A further refunctionalization of either *So*-NCC-2 (**5**) or *So*-NCC-3 (**6**) (or both) is suggested to result in the formation of the most polar of the *So*-NCCs, *So*-NCC-1 (**9**), which was detected in small amounts here and which displays a new constitution for an NCC (Kräutler and Matile 1999). While all of these indicated refunctionalization reactions clearly increase the polarity of the NCCs, a further attachment of a polar functionality, as observed with the *Bn*-NCCs (Mühlecker and Kräutler 1996) has not been detected here. Such refunctionalizations, as the malonylation of *Bn*-NCC-3 (**3c**) to *Bn*-NCC-1 (**3a**) (Hörtensteiner 1998a), have been considered to be of relevance for the transport and deposition of chlorophyll catabolites in the vacuoles (Hinder 1998; Lu et al. 1998; Tommasini 1998; Kräutler and Matile 1999). For the three main catabolites (**5**, **6** and **7**) an identification with *Cj*-NCC (**4**) or a chemically prepared derivative of **4** could be achieved. As seen earlier for oilseed rape, where three NCCs (the Bn-NCCs) appear to be closely related in catabolism (Mühlecker and Kräutler 1996) also for the senescent leaves of spinach, catabolic sequences can be suggested in which the less polar *So*-NCCs are converted to more polar ones.

The available information indicates a consistent stereochemistry at the chiral centres C(1), C(13^2) and C(15) in the *So*-NCCs **5**, **6** and **7**: they are all assigned to have the same configuration at these centers and also the same one as the catabolite from *C. japonicum* (*Cj*-NCC, **4**). The information from CD-spectra further suggests a common configuration of C(15) in all of the main NCCs isolated from barley, oil seed rape, *C. japonicum*, and spinach. This chiral center is suggested to arise from the hypothetical (enzymatic or non-enzymatic) final tautomerization of FCC-precursors to the corresponding NCCs. However, the NCC's (and the FCCs) fall into two classes with respect to the configuration at C(1) due to the presence of two types of reductases in higher plants that incorporate hydrogen at this chiral center (Rodoni et al. 1997; Hörtensteiner et al. 2000; Wüthrich et al. 2000). Therefore, the assignment of a common configuration at C(15) would indicate the tautomerization step to attach the hydrogen to C(15) with a common (diastereofacial) selectivity, irrespective of the configuration at C(1). The observed relative configuration at C(15) and C(13^2), with H-C(15) cis to the methoxycarbonyl group at C(13^2) in **1** and **5** (or a carboxyl group in **3a**) (Kräutler et al. 1991, 1992; Oberhuber et al. 2001) appears to be a general characteristic of the isolated NCCs. This structural aspect is likely to be the result of nonenzymatic equilibration reactions at the acidic C(13^2) position, which adjust its configuration to that at C(15). The latter process would be assumed to occur in the senescent plant leaf, but it also takes place in the isolated, dissolved NCCs.

Conclusion

The structures of a set of five nonfluorescent chlorophyll catabolites (NCCs) from senescent leaves of spinach have been (tentatively) characterized. The most abundant of the NCCs from spinach, of *So*-NCC-2 (**5**) (Oberhuber et al. 2001) was analyzed as a stereo-isomer of the nonfluorescent chlorophyll catabolite *Hv*-NCC-1 (**1**). This finding, first of all, underlined the relevance of extensive peripheral hydroxylations in the course of chlorophyll breakdown in higher plants under natural growth conditions. In addition, the epimeric nature at C(1) of *So*-NCC-2 (**5**) and of *Hv*-NCC-1 (**1**), as well as the identity of *Cj*-NCC (**4**) from *C. japonicum* and *So*-NCC-4 (**7**) from spinach, are consistent with the occurrence of two classes of RCC-reductases (Rodoni et al. 1997; Mühlecker et al. 2000; Hörtensteiner et al. 2000; Wüthrich et al. 2000; Oberhuber et al. 2001) in these higher plants. The constitutions of NCCs can now be delineated with little ambiguity (Kräutler et al. 1991; Kräutler and Matile 1999). We have also made some progress in the recent years towards establishing the pattern of the relative stereochemistry at the chiral centres of the reduced tetrapyrrolic skeleton (by means of chemical correlations of the NCCs from the same plant source as well as from different plant sources, see e.g. Oberhuber et al. 2001).

The identification of five *So*-NCCs has provided first evidence for the occurrence of several catabolic transformations on the level of the NCCs in a single senescent plant, involving three peripheral functionalities. The observation of the rather unpolar *So*-NCC's **8** and **7** indicate the peripheral functional groups of **5**

to be incorporated by two hydroxylation reactions of the nonpolar side chains at positions C(3) and C(8). Likewise, the simultaneous occurrence of the diacid *So*-NCC-3 (**6**) and of the mono-esters **7** and **8** points to a 'late' hydrolysis of the methyl ester functionality during chlorophyll breakdown. In spinach, this is likely to occur at the stage of the colourless NCCs, and not at that of the biosynthesis precursor pheophorbide *a*, as suggested elsewhere for the green alga *Chlamidomonas reinhardtii* (see e.g. Doi et al. 2001; Shioi et al. 1996). While the earlier phase of chlorophyll breakdown in higher plants was revealed to pass through a remarkably stringent entry point, the monooxygenation of pheophorbide a (Hörtensteiner et al. 1995, 1998b), the rather diverse structures of the NCCs, as displayed in senescent leaves of spinach, may indicate the later phases of this 'detoxification process' (Kräutler and Matile 1999) to follow less strictly regulated pathways.

Acknowledgements

We would like to thank C. Eichmüller, S. Ostermann, K.-H. Ongania, Walter Mühlecker for their important NMR-spectroscopic and mass spectrometric help and Alex Cowan (IGER, Aberystwyth) for samples of the spinach leaves. Financial support by the Austrian National Science Foundation (Project No. P 13503; B. K.) and by the Swiss National Science Foundation (S. H.) is gratefully acknowledged.

References

Bortlik K-H, Peisker C and Matile P (1990) A novel type of chlorophyll catabolite in senescent barley leaves. J Plant Physiol 136: 161–165

Brown SB, Houghton JD and Hendry GAF (1991) Chlorophyll breakdown. In: Scheer H (ed) Chlorophylls, pp 465–489. CRC Press, Boca Raton, Florida

Curty C and Engel N (1996) Detection, isolation and structure elucidation of a chlorophyll *a* catabolite from autumnal senescent leaves of *Cercidiphyllum japonicum*. Phytochemistry 42: 1531–1536

Doi M, Inage T and Shioi Y (2001) Chlorophyll degradation in a *Chlamydomonas reinhardtii* mutant: an accumulation of pyropheophorbide a by anaerobiosis. Plant Cell Physiol 42: 469–474

Ginsburg S and Matile P (1993) Identification of catabolites of chlorophyll porphyrin in senescent rape cotyledons. Plant Physiol 102: 521–527

Hendry GAF, Houghton JD and Brown SB (1987) The degradation of chlorophyll – a biological enigma. New Phytol 107: 255–302

Hinder B, Schellenberg M, Rodoni S, Ginsburg S, Vogt E, Martinoia E, Matile P and Hörtensteiner S (1996) How plants dispose of chlorophyll catabolites. Directly energized uptake of tetrapyrrolic breakdown products into isolated vacuoles. J Biol Chem 271: 27233–27236

Hörtensteiner S (1998a) NCC malonyltransferase catalyses the final step of chlorophyll breakdown in rape (*Brassica napus*). Phytochemistry 49: 953–956

Hörtensteiner S and Kräutler B (2000) Chlorophyll breakdown in oilseed rape. Photosynth Res 64: 137–146

Hörtensteiner S, Vicentini F and Matile P (1995) Chlorophyll breakdown in senescent cotyledons of rape, *Brassica napus* L.: enzymatic cleavage of phaeophorbide *a in vitro*. New Phytol 129: 237–246

Hörtensteiner S, Wüthrich KL, Matile P, Ongania K-H and Kräutler B (1998b) The key step in chlorophyll breakdown in higher plants. Cleavage of pheophorbide *a* macrocycle by a monooxygenase. J Biol Chem 273: 15335–15339

Hörtensteiner S, Rodoni S, Schellenberg M, Vicentini F, Nandi OI, Qiu Y-L and Matile P (2000) Evolution of chlorophyll degradation: the significance of RCC reductase. Plant Biol 2: 63–67

Ito H, Tanaka Y, Tsuji H and Tanaka A (1993) Conversion of chlorophyll *b* to chlorophyll *a* by isolated cucumber etioplasts. Arch Biochem Biophys 306: 148–151

Ito H, Ohysuka T and Tanaka A (1996) Conversion of chlorophyll *b* to chlorophyll *a via* 7-hydroxymethyl chlorophyll. J Biol Chem 271: 1475–1479

Iturraspe J, Moyano N and Frydman B (1995) A new 5-formylbilinone as the major chlorophyll *a* catabolite in tree senescent leaves. J Org Chem 60: 6664–6665

Kessler H, Gehrke M and Griesinger C (1988) Zweidimensionale NMR-Spektroskopie, Grundlagen und Übersicht über die Experimente. Angew Chem 100: 507–544; Angew Chem Int Ed Engl 27: 490–537

Kräutler B and Matile P (1999) Solving the riddle of chlorophyll breakdown. Acc Chem Res 32: 35–43

Kräutler B, Jaun B, Bortlik K-H, Schellenberg M and Matile P (1991) On the enigma of chlorophyll degradation: the constitution of a secoporphinoid catabolite. Angew Chem Int Ed Engl 30: 1315–1318

Kräutler B, Jaun B, Amrein W, Bortlik K, Schellenberg M and Matile P (1992) Breakdown of chlorophyll: constitution of a secoporphinoid chlorophyll catabolite isolated from senescent barley leaves. Plant Physiol Biochem 30: 333–346

Losey FG and Engel N (2001) Isolation and characterization of a urobilinogenoidic chlorophyll catabolite from *Hordeum vulgare*. J Biol Chem 276: 8643–8647

Lu Y-P, Li Z-S, Drozdowicz Y-M, Hörtensteiner S, Martinoia E and Rea PA (1998) AtMRP2, an *Arabidopsis* ATP binding cassette transporter able to transport glutathione S-conjugates and chlorophyll catabolites: functional comparisons with AtMRP1. Plant Cell 10: 267–282

Matile P (1987) Seneszenz bei Pflanzen und ihre Bedeutung für den Stickstoffhaushalt. Chimia 41: 376–381

Matile P and Kräutler B (1995) Wie und warum bauen Pflanzen das Chlorophyll *ab*. Chem unserer Zeit 29: 298–306

Matile P, Ginsburg S, Schellenberg M and Thomas H (1988) Catabolites of chlorophyll in senescing barley leaves are localized in the vacuoles of mesophyll cells. Proc Natl Acad Sci USA 85: 9529–9532

Matile P, Hörtensteiner S, Thomas H and Kräutler B (1996) Chlorophyll breakdown in senescent leaves. Plant Physiol 112: 1403–1409

Mendel G (1865) Versuche über Pflanzenhybriden. Verhandlungen des Naturwissenschaftlichen Vereins, Brünn 4: 3–47

Mühlecker W and Kräutler B (1996) Breakdown of chlorophyll: constitution of nonfluorescing chlorophyll-catabolites from senescent cotyledons of the dicot rape. Plant Physiol Biochem 34: 61–75

Mühlecker W, Kräutler B, Ginsburg S and Matile P (1993) Breakdown of chlorophyll: the constitution of a secoporphinoid chlorophyll catabolite from senescent rape leaves. Helv Chim Acta 76: 2976–2980

Mühlecker W, Ongania K-H, Kräutler B, Matile P and Hörtensteiner S (1997) Tracking down chlorophyll breakdown in plants: elucidation of the constitution of a fluorescent chlorophyll catabolite. Angew Chem Int Ed Engl 36: 401–404

Mühlecker W, Kräutler B, Moser D, Matile P and Hörtensteiner S (2000) Breakdown of chlorophyll: a fluorescent chlorophyll catabolite from sweet pepper (*Capsicum annuum*). Helv Chim Acta 83: 278–286

Oberhuber M, Berghold J, Mühlecker W, Hörtensteiner S and Kräutler B (2001) Chlorophyll breakdown – on a nonfluorescent chlorophyll catabolite from spinach. Helv Chim Acta 84: 2615–2627

Pretsch E, Bühlmann P and Affolter C (2000) Structure Determination of Organic Compounds, pp 158–160. Springer-Verlag, Berlin

Rodoni S, Vicentini F, Schellenberg M, Matile P and Hörtensteiner S (1997) Partial purification and characterization of red chlorophyll catabolite reductase, a stroma protein involved in chlorophyll breakdown. Plant Physiol 115: 677–682

Sanders JKM and Hunter BK (1987) Modern NMR-spectroscopy. Oxford University Press, Oxford

Scheer H (ed) (1991) Chlorophylls. CRC-Press, Boca Raton, Florida

Scheumann V, Ito H, Tanaka A, Schoch S and Rüdiger W (1996) Substrate specificity of chlorophyll(ide) *b* reductase in etioplasts of barley (*Hordeum vulgare*). Eur J Biochem 242: 163–170

Scheumann V, Schoch S and Rüdiger W (1999) Chlorophyll *b* reduction during senescence of barley seedlings. Planta 209: 364–370

Shioi Y, Watanabe K and Takamiya K (1996) Enzymatic conversion of pheophorbide *a* to a precursor of pyropheophorbide *a* in leaves of *Chenopodium album*. Plant Cell Physiol 37: 1143–1149

Smith RD, Light-Wahl KJ, Winger BE and Goodlett DR (1995) Electrospray Ionization. In: Matsuo T, Caprioli RM, Gross ML and Seyama Y (eds) Biological Mass Spectrometry: Present and Future, pp 41–74. John Wiley & Sons, Chichester, UK

Tommasini R, Vogt E, Fromenteau M, Hörtensteiner S, Matile P, Amrhein N and Martinoia E (1998) An ABC transporter of *Arabidopsis thaliana* has both glutathione-conjugate and chlorophyll catabolite transport activity. Plant J 13: 773–780

Watson TR (1995) Fast atom bombardment. In: Matsuo T, Caprioli RM, Gross ML and Seyama Y (eds) Biological Mass Spectrometry: Present and Future, pp 24–40. John Wiley & Sons, Chichester, UK

Wüthrich KL, Bovet L, Hunziker PE, Donnison IS and Hörtensteiner S (2000) Molecular cloning, functional expression and characterisation of RCC reductase involved in chlorophyll catabolism. Plant J 21: 189–198